Measurement 43 (2010) 1447–1457

Contents lists available at ScienceDirect

Measurement

journal homepage: www.elsevier.com/locate/measurement

A hybrid unscented filtering and particle swarm optimization technique for harmonic analysis of nonstationary signals

P.K. Dash [a,*], Shazia Hasan [a], B.K. Panigrahi [b]

[a] Siksha 'O' Anusandhan University, Bhubaneswar 751 030, India
[b] Indian Institute of Technology, New Delhi, India

ARTICLE INFO

Article history:
Received 11 June 2009
Received in revised form 14 August 2010
Accepted 25 August 2010
Available online 31 August 2010

Keywords:
Frequency estimation
Time-varying harmonics
Harmonics estimation
Unscented transformation
Unscented Kalman filter
Adaptive particle swarm optimization

ABSTRACT

This paper presents a modified unscented Kalman filter for accurate estimation of frequency and harmonic components of a time-varying signal embedded in noise with low signal-to-noise ratio. Further, the model and measurement error covariances along with the unscented Kalman filter parameters are selected using a modified particle swarm optimization algorithm. To circumvent the problem of premature convergence and local minima, a dynamically varying inertia weight based on the variance of the population fitness is used. This results in a better local and global searching ability of the particles, which improves the convergence of the velocity and better accuracy of the unscented Kalman filter parameters. Various simulation results for nonstationary sinusoidal signals with time varying amplitude, phase and harmonic content corrupted with noise, reveal significant improvement in noise rejection and speed of convergence and accuracy in comparison to the well known extended Kalman filter.

1. Introduction

The problem of estimating frequency and other parameters of sinusoidal signal in white noise in radar, nuclear magnetic resonance, power networks etc., have been extensively studied. Amongst the several methods for frequency, amplitude and phase estimation of nonstationary signals, Discrete Fourier Transform (DFT), and Fast Fourier Transform (FFT) are widely used [1–3]. However, both the above methods suffer from aliasing, leakage, and picket fence effects and hence need error compensation and adaptive window width [4]. Some of the known signal processing techniques like artificial neural networks [5,6], adalines [7–9], linear prediction technique [10], adaptive filters [11], supervised Gauss–Newton algorithm [12,13], least-error squares and its variants [14–17], extended Kalman filters [18–20], have been used for time-varying signal parameter estimation. Most of these algorithms require heavy computational outlay and suffer from inaccuracies in the presence of noise with low signal-to-noise ratio (SNR).

Recently, a novel unscented Kalman filter (UKF) [21–25] has been proposed to overcome the shortcoming of the extended Kalman filter (EKF) algorithm for its instability due to linearization, erroneous parameters, costly calculations of derivatives, and the biased nature of the estimates. The main advantage of the unscented transformation used in UKF is that it does not use linearization for computing the state and error covariance matrices resulting in a more accurate estimation of the parameters of a nonstationary signal. However, its accuracy significantly reduces, if SNR is low and the noise covariances and some of the parameters used in unscented transformation are not chosen correctly. Thus for best signal tracking performance, it is proposed in this paper to use adaptive particle swarm optimization technique, which is found to be superior to the conventional particle swarm optimization (PSO) [26–29] for the optimal choice of UKF parameters and error covariances.

* Corresponding author. Tel.: +91 674 2350653; fax: +91 674 2350642.
E-mail address: pkdash.india@gmail.com (P.K. Dash).

0263-2241/$ - see front matter © 2010 Elsevier Ltd. All rights reserved.
doi:10.1016/j.measurement.2010.08.013

Nomenclature

Symbols

$\mathbf{A}_n$	state transition matrix
a_n	amplitude of the nth harmonic sinusoidal signal
F_i	fitness of the ith particle
F_{avg}	average fitness of the population
F_n	normalizing factor
f_s	sampling frequency
$\hat{g}best$	global best position
$\mathbf{H}_k$	measurement transition vector
$\mathbf{K}_k$	Kalman gain
K	constriction factor
k	time instant
L	dimension of the state vector
N	order of the harmonic
$\mathbf{P}_0$	covariance of the state vector
$pbest_i$	local best value of the ith particle
$\mathbf{Q}$	model error covariance
R	measurement error covariance
T_s	sampling time
$\overline{V}(t)$	mean velocity of the particle
$\overline{V}(k)$	velocity of the particle
$V_i(k+1)$	velocity of the ith particle at time instant $k+1$
$\mathbf{v}_k$	model noise
$W_i^{(m)}$	mean weight factor
$W_i^{(c)}$	covariance weight factor
w	inertia weight factor
$\mathbf{X}_k$	state vector
$x_i(k+1)$	position of the ith particle at time instant $k+1$
$\hat{\mathbf{x}}_k^-$	weighted mean of the sigma points
$\hat{\mathbf{x}}_0$	mean of the state vector
$\mathbf{Y}_{i,k\|k-1}$	transformed sigma point output
$\hat{y}_k^-$	weighted mean of the sigma point outputs
y_k	measurement at time instant k
α	constant
β	prior knowledge of the distribution of the state vector
η_k	measurement noise
κ	scaling parameter
λ	scaling parameter
μ	forgetting factor
$\mu_B(x)$	membership function of set big
$\mu_S(x)$	membership function of set small
ρ	forgetting factor
σ^2	variance of the fitness of the particles
$\Delta\sigma$	change in standard deviation
ϕ_1	acceleration coefficient
ϕ_2	acceleration coefficient
φ_n	phase of the nth sinusoidal signal
$\boldsymbol{\chi}$	sigma point matrix
ω	angular frequency of the fundamental sinusoidal signal

Acronyms

APSO	adaptive particle swarm optimization
EKF	extended Kalman filter
MPSO	modified particle swarm optimization
MSE	mean square error
PSO	particle swarm optimization
UKF	unscented Kalman filter

The particle swarm optimization technique is a stochastic optimization technique developed by Eberhert and Kennedy that stimulates the social behaviors of birds or fish. Although PSO is easy to implement and has few parameters to adjust, it suffers from premature convergence, velocity explosion, and finding good solutions as quickly as it could. To circumvent this problem, an alternative approach of dynamically varying the inertia weight randomly based on the variance of the population fitness is chosen. This results in a better local and global searching ability of the particles, which improves the convergence of the velocity and better accuracy of the UKF parameters. Two different approaches for inertia weight variation are presented in this paper known as modified particle swarm optimization (MPSO) and adaptive particle swarm optimization (APSO). A method of dynamically varying the inertia weight based on fuzzy logic using just two rules is presented in this paper for tuning the UKF parameters, and this algorithm is termed simply as APSO. Several simulation results for nonstationary power signals corrupted with noise having low SNR reveal significant estimation accuracy with optimized UKF parameters.

2. Unscented Kalman filter (UKF)

Although EKF is straightforward and simple it suffers from instability due to linearization and erroneous parameters, costly calculation of Jacobean matrices, and the biased nature of its estimates [17–21]. The UKF is considered in this paper to overcome the disadvantages of EKF. The UKF belongs to the family of sigma-point filters and uses an unscented transformation that computes the statistics of a random variable undergoing nonlinear transformation. The main advantage of UKF is that it does not use linearization for calculating the state predictions, covariance matrices and thus it provides accurate Kalman gain estimates. Instead of linearizing the Jacobean matrices, the UKF uses a deterministic sampling approach to capture mean and covariance estimates with a minimal set of $2 \times L + 1$, sigma points (L is the state dimension) based on a square-root decomposition of the prior covariance [22]. These sigma points are propagated through the nonlinearity, without approximation, and a weighted mean and covariance is found. Like the EKF, the UKF uses a recursive algorithm that uses the system model, measurements, and known statistics of the noise mixed with the signal. The UKF was originally designed to estimate the states of a dynamic system and for nonlinear control applications [21–25]. In this paper the UKF is used to track the fundamental and harmonic components of a nonstationary signal that is found in power networks.

The signal for estimation of time-varying frequency and harmonics is represented by the following discretized equation:

$$y_k = \sum_{n=1}^{N} a_n \sin\left(2\pi n \frac{f_0}{f_s} k + \phi_n\right) + \eta_k \quad (1)$$

where y_k is the measured signal, a_n is the time-varying peak amplitude of the nth harmonic component of the signal, N is the order of the harmonic, f_0 is frequency of the fundamental component, and f_s is the sampling frequency. In Eq. (1), η_k represents measurement noise with associated variance. The signal and observation models are derived in state space form as follows:

$$\mathbf{x}_k = f(\mathbf{x}_{k-1}) + \mathbf{v}_k \quad (2)$$

where the state vector $\mathbf{x}$ is given by $\mathbf{x}_k = [a_1 \sin\phi_1\ a_1\cos\phi_1 \ldots a_n \sin\phi_n a_n \cos\phi_n \omega]^T$, angular frequency $\omega = 2\pi f_0$, and

$$f(\mathbf{x}_k) = \mathbf{A}_{nk}\mathbf{x}_k^T \quad (3)$$

The state transition matrix

$$\mathbf{A}_{nk} = \begin{bmatrix} \mathbf{A}_1 & 0 & 0 & 0 \\ 0 & \ddots & 0 & \\ 0 & \mathbf{A}_n & 0 & \\ 0 & 0 & 1 & \end{bmatrix}, \quad (4)$$

where

$$\mathbf{A}_n = \begin{bmatrix} \cos(n\omega k T_s) & \sin(n\omega k T_s) \\ -\sin(n\omega k T_s) & \cos(n\omega k T_s) \end{bmatrix} \quad (5)$$

The model error covariance matrix for this signal is

$$\mathbf{Q} = E\begin{bmatrix}\mathbf{v} & \mathbf{v}^T\end{bmatrix} = q\mathbf{I}, \mathbf{I} \text{ is a unit matrix of order } N+1 \quad (6)$$

The measurement model for the signal represented by Eq. (1) is obtained as

$$y_k = \mathbf{H}_k\mathbf{x}_k + \eta_k \quad (7)$$

where

$$\mathbf{H}_k = [1010\ldots100], \quad (8)$$

and the measurement error covariance $R = E[\eta\eta^T]$.

Given a state vector at step $k-1$, sigma points are computed and stored in the columns of $L \times (2L+1)$ sigma point matrix $\boldsymbol{\chi}_{k-1}$ where L = dimension of the state vector. For the estimation of fundamental signal frequency, amplitude and phase without modeling the harmonics, $L = 3$ and thus $\boldsymbol{\chi}_{k-1}$ is a 3×7 matrix. However, for the estimation of N number of harmonics and the fundamental frequency $L = 2N+1$, thus $\boldsymbol{\chi}_{k-1}$ is a $(2N+1)(4N+3)$ matrix.

The UKF algorithm is summarized in the following steps:

1. Initialization

For the system state $\mathbf{x}$, initialized with

$$\hat{\mathbf{x}}_0 = E[\mathbf{x}_0], \quad \mathbf{P}_0 = E[(\mathbf{x}_0 - \hat{\mathbf{x}}_0)(\mathbf{x}_0 - \hat{\mathbf{x}}_0)^T], \quad (9)$$

2. Time update

Given a state vector at time step $k-1$, sigma points are computed and stored in the columns of $L \times (2L+1)$ sigma point matrix $\boldsymbol{\chi}$. For the present problem, $L = 3$ so $\boldsymbol{\chi}_{k-1}$is a 3×7 matrix. The sigma points are computed as

$$\boldsymbol{\chi}_{0,k-1} = \hat{\mathbf{x}}_{k-1},\ i = 0,\ \boldsymbol{\chi}_{i,k-1} = \hat{\mathbf{x}}_{k-1} + \left(\sqrt{(L+\lambda)\mathbf{P}_{k-1}}\right)_i,$$
$$i = 1,2,\ldots,L\boldsymbol{\chi}_{i+L,k-1} = \hat{\mathbf{x}}_{k-1} - \left(\sqrt{(L+\lambda)\mathbf{P}_{k-1}}\right)_i,$$
$$i = L+1,\ldots,2L \quad (10)$$

and $\left(\sqrt{(L+\lambda)\mathbf{P}_{k-1}}\right)_i$ is the ith column of the matrix square root [22,23] of $(L+\lambda)\mathbf{P}_{k-1}$. The parameter λ is used to control the covariance matrix, and is given by

$$\lambda = \alpha^2(L+\kappa) - L \quad (11)$$

Both λ and κ are scaling parameters that determine the spread of the sigma points. The constant α determines the spread of the sigma points around $\hat{\mathbf{x}}$ and is usually set to $e^{-4} \leqslant \alpha \leqslant 1$.

After computing the sigma points the time update of state estimates are given by

$$\boldsymbol{\chi}_{k/k-1} = f(\boldsymbol{\chi}_{k-1}),\ \text{and}\ \hat{\mathbf{x}}_k^- = \sum_{i=0}^{2L} W_i^m \boldsymbol{\chi}_{i,k|k-1} \quad (12)$$

where the weights $W_i^{(m)}$ are defined by

$$W_0^{(m)} = \frac{\lambda}{L+\lambda}, \quad W_i^{(m)} = \frac{\lambda}{2(L+\lambda)},$$
$$W_{i+L}^{(m)} = \frac{1}{2(L+\lambda)},\ i = 1,\ldots,L \quad (13)$$

The a priori error covariance is given by

$$\overline{\mathbf{P}}_\mathbf{k} = \sum_{\mathbf{i=0}}^{\mathbf{2L}} \mathbf{W}_\mathbf{i}^{(\mathbf{c})}[\boldsymbol{\chi}_{\mathbf{i,k|k-1}} - \hat{\mathbf{x}}_\mathbf{k}^-][\boldsymbol{\chi}_{\mathbf{i,k|k-1}} - \hat{\mathbf{x}}_\mathbf{k}^-]^\mathbf{T} + \mathbf{Q}_\mathbf{k} \quad (14)$$

$$W_0^{(c)} = \frac{\lambda}{(L+\lambda)} + (1-\alpha^2+\beta), \quad W_i^{(c)} = \frac{1}{2(L+\lambda)} + (1-\alpha^2+\beta),$$
$$W_{i+L}^{(c)} = \frac{1}{2(L+\lambda)},\ i = 1,\ldots,L \quad (15)$$

The estimated output

$$\mathbf{Y}_{i,k|k-1} = \mathbf{H}_k\boldsymbol{\chi}_{i,k|k-1},\ \text{and}\ \hat{y}_k^- = \sum_{i=0}^{2L} W_i^{(m)}\mathbf{Y}_{i,k|k-1} \quad (16)$$

The a posterior state estimate $\hat{\mathbf{x}}_k$, and the Kalman gain $\mathbf{K}_k$ are computed as

$$\hat{\mathbf{x}}_k = \hat{\mathbf{x}}_k^- + \mathbf{K}_k(y_k - \hat{y}_k^-),\ \text{and}\ \mathbf{K}_k = \mathbf{G}_k S_k^{-1} \quad (17)$$

where

$$\mathbf{G}_k = \sum_{i=0}^{2L} W_i^{(c)}[\boldsymbol{\chi}_{i,k|k-1} - \hat{\mathbf{x}}_k^-][\mathbf{Y}_{i,k|k-1} - \hat{y}_k^-]^T, \quad (18)$$

and

$$S_k = \sum_{i=0}^{2L} W_i^{(c)}[Y_{i,k|k-1} - \hat{y}_k^-][\mathbf{Y}_{i,k|k-1} - \hat{y}_k^-]^T + R_k \quad (19)$$

R_k is the measurement error covariance. The a posterior estimate of the error covariance matrix is given by

$$\mathbf{P}_k = [\overline{\mathbf{P}}_\mathbf{k}]^{-\mathbf{1}} - \mathbf{K}_\mathbf{k}\mathbf{S}_\mathbf{k}\mathbf{K}_\mathbf{k}^\mathbf{T} \quad (20)$$

2.1. Tuning of the unscented Kalman filter error covariances

Current implementations of the UKF for signal parameter estimation have considered the model error and measurement error covariances as constant and determined apriori [22–24]. Usually a small value for $\mathbf{Q} = qI$ (q = 0.0001, I = unit matrix of appropriate dimension) is adopted for most of the filter computations. In this paper a self-tuning procedure for adapting the covariances is presented for improving the performance of the filter during sudden changes in the amplitude, phase, or the frequency of the signal. The model error is estimated as

$$\mathbf{v}_k = f(\hat{\mathbf{x}}_k) - f(\hat{\mathbf{x}}_k^-) = \mathbf{K}_k(y_k - \hat{y}_k^-) \tag{21}$$

Using Eqs. (18) and (19), the value of process covariance matrix is updated as the average of the variance square during the successive iterations. Thus the incremental matrix $\mathbf{Q}_k$ is obtained as

$$\mathbf{Q}_k = (1/2)\left\{\left(K_k\left(y_k - \sum_{i-0}^{2L} W_i^{(m)}\mathbf{Y}_{i,k|k-1}\right)\right)^2 + \left(\mathbf{K}_k\left(y_k - \sum_{i-0}^{2L} W_i^{(m)}\mathbf{Y}_{i,k-1|k-2}\right)\right)^2\right\} \tag{22}$$

However, if the value of $\mathbf{Q}_k$ obtained from Eq. (25) is sufficiently large, the modified UKF can tolerate high order error in the unscented transformation by enlarging the noise covariance matrix, and thereby improving the stability, but resulting in a large estimation error. Therefore, a threshold value of $\mathbf{Q}_k$ is required to provide both, the accuracy and stability in tracking harmonic signals. Further the initial value of $\mathbf{Q}_k$ can be chosen using PSO algorithm as outlined in the next section. In a similar way the measurement error covariance is updated as

$$R_k = \rho R_{k-1} + (1-\rho)\left(y_k - \sum_{i-0}^{2L} W_i^{(m)}\mathbf{Y}_{i,k|k-1}\right)^2 \tag{23}$$

ρ is a forgetting factor and is taken as =0.9. The values of system state $\hat{\mathbf{x}}_k$ and covariance matrix $\mathbf{P}_k$ become the input of the successive prediction-correction loop. Through a proper choice of the sigma points, that is the parameters α, λ, β and the initial values of the covariances $\mathbf{Q}$ and R, the UKF assures a better performance than the EKF in estimating fundamental frequency, and amplitude and phase of the fundamental and harmonic components of a signal buried in noise. Thus to improve the performance of UKF, a stochastic optimization technique like the PSO [26–29] and its variants are used to obtain the parameters α, λ, β, $\mathbf{Q}$, and R instead of trial and error approach. Here the objective function is chosen as

$$O_{bji} = (1/M)\sum_{k=1}^{M}(y_k - \hat{y}_k^-)^2 \tag{24}$$

and the fitness of the ith particle is

$$F_i = \frac{1}{1 + O_{bji}} \tag{25}$$

where M is the number of samples chosen for determining the mean square error (MSE). The optimization is aimed at minimizing the MSE or maximizing the fitness value.

3. Adaptive particle swarm optimization of UKF algorithm

A solution to obtain an optimal performance with low SNR can be possible using particle swarm optimization technique. PSO is a novel stochastic origin in the motion of a flock of birds searching for food. The basic PSO algorithm is started by scattering a number of particles called swarms in the function search space. Each particle moves in the search space looking for the global minimum or maximum. During its flight each particle adjusts its trajectory by dynamically altering its velocity according to its own flying experience and the flying experience of the other particles in the search space. The PSO approach is becoming very popular due to its simplicity of implementation and its ability to quickly converge to a reasonably good solution. For a particle moving in a multidimensional search space let x_{ij} and V_{ij} denotes the position of ith particle in the jth dimension and velocity at time k. The local best value in PSO is computed as

$$pbest_i(k+1) = \begin{cases} pbest_i(k), & \text{if } F(x_i(k+1)) > F(pbest_i(k)) \\ x_i(k+1), & \text{if } F(x_i(k+1)) < F(pbest_i(k)) \end{cases} \tag{26}$$

where F stands for the fitness function of the moving particles and the global best position is obtained as

$$gbest(k) = \min\{F(pbest_0(k)), F(pbest_1(k)), F(pbest_2(k)), \ldots, F(pbest_s(k))\} \tag{27}$$

The modified velocity and position of each particle at time $(k+1)$ can be calculated as

$$V_i(k+1) = K\{wv_i(k) + \varphi_1 r_1(pbest_i(k) - x_i(k)) + \varphi_2 r_2(gbest(k) - x_i(k))\} \tag{28}$$

$$x_i(k+1) = x_i(k) + V_i(k+1) \tag{29}$$

where V_i is the velocity of ith particle at time $k+1$, x_i is the current position, w is the inertia weight factor ϕ_1 and ϕ_2 are acceleration constant, r_1 and r_2 are two random numbers in the range [0, 1], K is a constriction factor and is obtained as

$$K = \frac{2}{|2 - \varphi - \sqrt{\varphi^2 - 4\varphi}|}, \text{and} \quad \varphi = \varphi_1 + \varphi_2; \;\; \varphi > 4 \tag{30}$$

A suitable selection of inertial weight w and acceleration coefficients ϕ_1 and ϕ_2 is crucial in providing a balance between the global and local search in the flying space. The particle velocity at any instant is limited to a chosen $V_{\max}$, which if too high will result in allowing the particles to fly past good solutions. On the other hand if $V_{\max}$ is too small, particles end up in local solutions only. The acceleration factors ϕ_1 and ϕ_2 used in Eq. (28) are varied according to the following equations:

$$\varphi_1 = (\varphi_{1\max} - \varphi_{1i}) \cdot \frac{iter}{iter_{\max}} + \varphi_{1i},$$

$$\varphi_2 = (\varphi_{2\max} - \varphi_{2i}) \cdot \frac{iter}{iter_{\max}} + \varphi_{2i} \tag{31}$$

The acceleration factors ϕ_1 and ϕ_2 are varied from 2.5 to 0.5, respectively to find out the best ranges for optimum solution. Although the conventional PSO can produce

optimal solutions of UKF parameters, it still suffers from premature convergence and gets stuck in local minima. Besides it suffers from an ineffective exploration strategy around local minima and therefore a change in particle motion methodology may speed up the search by improving exploration. Although there are several possible approaches for modifying the inertia weight iteratively, two approaches namely the modified PSO (MPSO) and the adaptive PSO (APSO) are presented below:

3.1. Modified PSO algorithm (MPSO)

The inertia weight is updated by finding the variation of the population fitness as

$$\sigma^2 = \sum_{i=1}^{M} \left(\frac{F_i - Favg}{F_n} \right)^2, \tag{32}$$

and

$$F_n = \{\max(|F_i - Favg|)\}, \quad i = 1, 2, 3 \ldots\ldots M \tag{33}$$

where *Favg* is the average fitness of the population of particles in a given generation; F_i is the fitness of the ith particle in the population; M is the total number of particles.

In Eq. (34), F_n is a normalizing factor, which is used to limit the value of the standard deviation σ. If σ is large, the population will be in a random searching mode, while for small σ or $\sigma = 0$, the solution tends towards a premature convergence and will give the local best position of the particles. To circumvent this phenomenon and to obtain *gbest* solution, the inertia weight factor is updated as

$$w(k) = \mu w(k-1) + (1-\mu)\sigma^2 \tag{34}$$

The forgetting factor μ is chosen as 0.9 for faster convergence. Another alternative form will be

$$w(k) = \mu_1 w(k-1) + r_3/2, \text{ and } 0 \leqslant \mu_1 \leqslant 0.5 \tag{35}$$

where r_3 is a random number in the range $[0, 1]$. Besides the influence of the past velocity of a particle on the current velocity is chosen to be random and the inertia weight is adapted randomly depending on the variance of the fitness value of a population. This result is an optimal coordination of local and global searching abilities of the particles.

3.2. Adaptive PSO algorithm (APSO)

In this algorithm the inertia weight factor is updated using fuzzy rule base and fuzzy membership values of the change in standard deviation $\Delta\sigma$ in the following way: The fuzzy sets chosen for $|\Delta\sigma|$ are B (Big) and S (Small) and are shown in Fig. 1a. The fuzzy rule base is formed in the following way:

Change in standard deviation

$$\Delta\sigma = \sigma(k) - \sigma(k-1) \tag{36}$$

The fuzzy rule base for arriving at a weight change is expressed as

R1.If $|\Delta\sigma|$ is B Then $\Delta w = r_4 \cdot \Delta\sigma$ (37)

R2 : If $|\Delta\sigma|$ is S Then $\Delta w = r_5 \Delta\sigma$

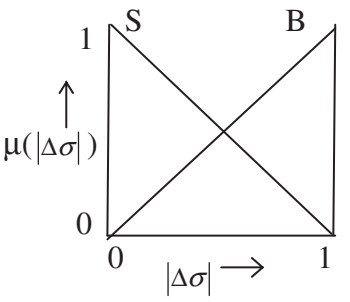

Fig. 1a. Membership function for $|\Delta\sigma|$.

where the membership functions for fuzzy sets B and S are given by

$$\mu_B(x) = |\Delta\sigma|; \text{ and } \mu_S(x) = 1 - |\Delta\sigma| \tag{38}$$

where r_4 and r_5 are random numbers between 0 and 1, and $0 \leqslant |\Delta\sigma| \leqslant 1$

Using centroid defuzzification principle the value of Δw is obtained as

$$\Delta w = |\Delta\sigma| r_4 \Delta\sigma + r_5 \Delta\sigma (1 - |\Delta\sigma|) \tag{39}$$

Thus the value of the new weight w is

$$w(k) = w(k-1) + \Delta w, \text{and } 0.4 \leqslant w(k) \leqslant 0.9 \tag{40}$$

In the above formulation the influence of the past velocity of a particle on the current velocity is chosen to be random and the inertia weight is adapted randomly depending on the variance of the fitness value of a population. This results in an optional coordination of local and global searching abilities of the particles. To run the PSO algorithm for optimizing the parameters α, q, and R, 20 particles for each of these parameters are chosen. For a given signal superimposed with 20 dB noise, the error between the measured signal and the estimated one is computed for each of these particles over a period of 2.5 cycles, i.e. 100 samples. From the individual error at each sampling instant, the total error for all the 100 samples is computed and is used to find the fitness function of a given particle, which is used for updating the position and velocity of the particle iteratively. The pseudo code for the PSO algorithm is given below:

Pseudo code for the proposed algorithm

```
Randomly initialize the velocities and positions of all
    the particles, and initialize w, λ and β
WHILE (the termination condition is not met)
Obtain the fitness function of individual particle using
    equation (25)
Obtain standard deviation σ using equations (32) and
    (33)
Compute pbest and gbest using equations (26) and (27)
Obtain |Δσ| and Δw using equations (36) and (39)
Update inertia weight using (40)
Update the velocities and positions of all the particles
END WHILE
```

4. Computer simulation and experimental results

To evaluate the performance of the proposed estimation technique, several simulation examples are given below along with the tables showing the absolute error (AE) in estimation for the harmonic components.

4.1. Static signal parameters

The test power signal is assumed to comprise a fundamental and several harmonics and is shown in Eq. (43) as

$$y(k) = 1.2 * \sin(\omega k T_s + \phi_1) + 0.25 * \sin(3\omega k T_s + \phi_3) + 0.15 * \sin(5\omega k T_s + \phi_5) + 0.1 * \sin(11\omega k T_s + \phi_{11}) + \eta(k) \quad (41)$$

The amplitude, phase, and the frequency of the signal are considered to be time-invariant and the sampling frequency is chosen as 2 kHz (40 samples per cycle on a 50 Hz base). Since it is required to estimate nine parameters of the signal, the value of L is set equal to 9, and thus the number of sigma points for this estimation are $2L + 1$, i.e. 19 and the augmented state vector $\boldsymbol{\chi}_{k-1}$ is a 9×19 matrix.

For optimizing the UKF performance, the PSO parameters are initialized with a population of 20 particles and the dimension chosen is 3. Out of the five UKF parameters β and κ are chosen as $\beta = 2$, $\kappa = 0$, and the other three namely α, $\mathbf{Q}$, and R are to be optimized. Here $\mathbf{Q} = q\mathbf{I}_{9\times 9}$, $\mathbf{I}$ is a 9th order unit matrix, and hence the variable q is to be optimized. For the conventional PSO algorithm, the initial values of the parameters ϕ_1, ϕ_2, $w_{\max}$, $w_{\min}$ are chosen as $\phi_1 = 2.1$, $\phi_2 = 2.1$, $w_{\max} = 0.9$, $w_{\min} = 0.4$. For the UKF, the lower and upper bound of α, q and R are chosen as $\alpha_{lower} = 0.01$, $q_{lower} = 0.001$, $R_{lower} = 0.001$, $\alpha_{upper} = 0.5$, $q_{upper} = 0.5$, $R_{upper} = 0.5$. The chosen fitness function is given in Eq. (25). A white Gaussian noise of SNR 20 dB is added to the test signal. Table 1 shows the absolute error (AE) of fundamental frequency, amplitude and phase of different harmonic components. From this table it is quite evident that the performance of the EKF algorithm is the worst in comparison to UKF and optimized UKF algorithms. Figs. 1b and 1c describe the convergence analysis of different variants of PSO for 20 dB and 30 dB noise, respectively. Also from Figs. 1b and 1c it is observed that out of the two variants of the PSO algorithm, the adaptive PSO (APSO) converges faster and gives lesser estimation error. The Test signal with 20 dB noise is shown in Fig. 2a, and the tracking performance of UKF, and its optimized variants MPSO, and APSO is shown in Figs. 2b and 2c, respectively. From these figures it is found that the APSO produces significantly better estimation accuracy in amplitude and phase for the 3rd and 5th harmonic components in comparison to UKF alone. Similar estimation error is observed for other harmonic components.

The succeeding sections describe the amplitude, and frequency variations in the fundamental and harmonic components of the signal described in Eq. (41) and their effects on the estimation accuracy.

Table 1
Absolute error of the signal with no change in signal parameter with 20 dB noise.

Order of harmonic	EKF	UKF	MPSO	APSO
Fundamental freq. error (Hz)	0.2505	0.2092	0.0972	0.005
Fundamental amp. error (pu)	0.066	0.052	0.032	0.010
3rd Harmonic amp. z error (pu)	0.15	0.098	0.087	0.012
5th Harmonic amp. error (pu)	0.115	0.025	0.0157	0.0021
11th Harmonic amp. error (pu)	0.053	0.039	0.0175	0.0170
Fundamental phase error	0.054	0.021	0.0171	0.0153
3rd Harmonic phase error	0.061	0.027	0.0191	0.0179
5th Harmonic phase error	0.066	0.035	0.022	0.0213
11th Harmonic phase error	0.069	0.037	0.0231	0.0221

4.2. Linear frequency variation

The fundamental frequency of the signal is varied linearly from the initial value of 50–65 Hz within a span of two

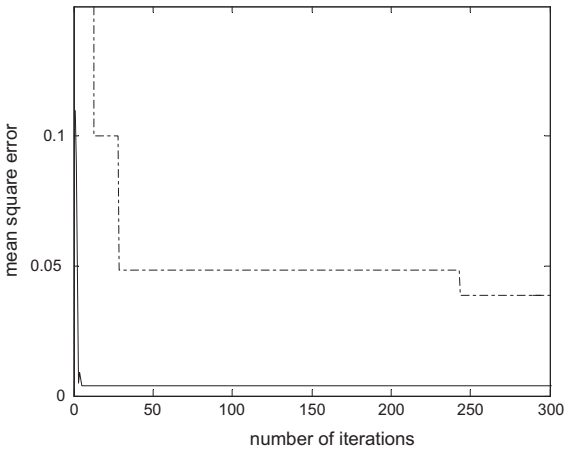

Fig. 1b. Convergence analysis of different variants of PSO with 20 dB noise. —, APSO; – – –, MPSO.

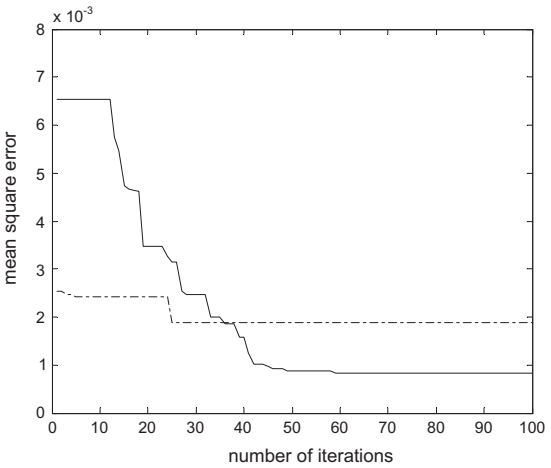

Fig. 1c. Convergence analysis of different variants of PSO with 30 dB noise. —, APSO; – – –, MPSO.

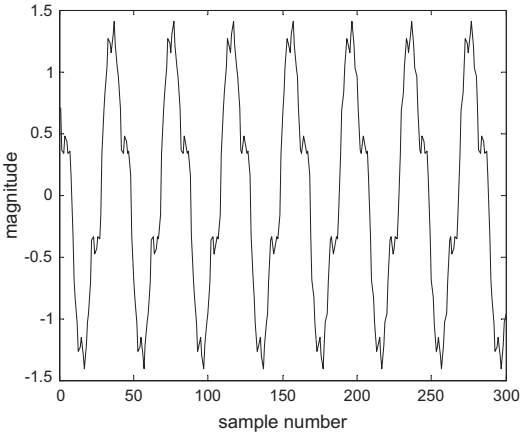

Fig. 2a. Test signal with constant parameters and 20 dB noise.

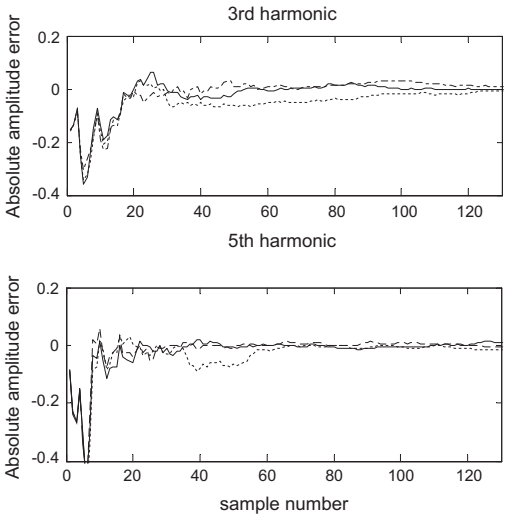

Fig. 2b. Comparison of 3rd and 5th harmonic amplitude error with 20 dB noise. - - - -, UKF; – – –, MPSO; —, APSO.

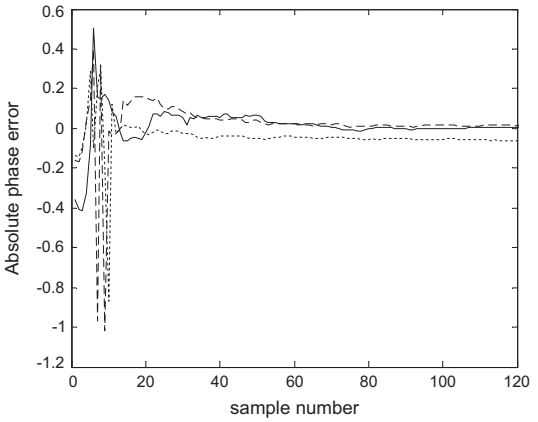

Fig. 2c. Comparison of 3rd harmonic phase error with 20 dB noise. - - - -, UKF; – – –, MPSO; —, APSO.

cycles and a similar frequency variation is generated in the harmonic components with a white Gaussian noise of SNR = 20 dB added to the signal given in Eq. (42). Further its angular frequency is varied in the following way:

$$\text{For } 0 \leqslant k \leqslant 100, \quad \omega = \omega_0; \text{ for } 100 \leqslant k \leqslant 200,$$
$$\omega = \omega_0 + \frac{\omega_1 - \omega_0}{100}(k - 100); \text{ for } k \geqslant 200 \quad \omega = \omega_1 \quad (42)$$

Table 2
Absolute error of linear frequency variation with 20 dB noise.

Order of harmonic	EKF	UKF	MPSO	APSO
Fundamental freq. error (Hz)	0.3031	0.2953	0.2412	0.0063
Fundamental amp. error (pu)	0.089	0.073	0.069	0.0131
3rd Harmonic amp. error (pu)	0.22	0.179	0.098	0.0119
5th Harmonic amp. error (pu)	0.133	0.0304	0.0272	0.0031
11th Harmonic amp. error (pu)	0.0675	0.0479	0.0285	0.0179

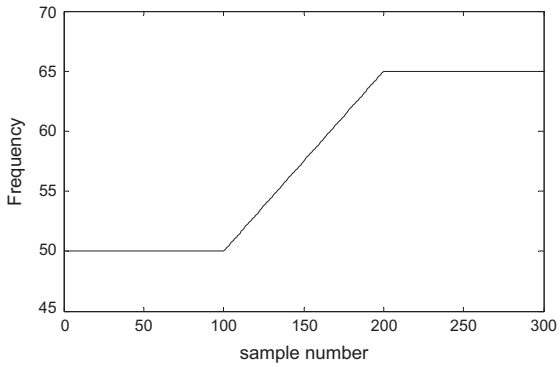

Fig. 3a. Ramp frequency change.

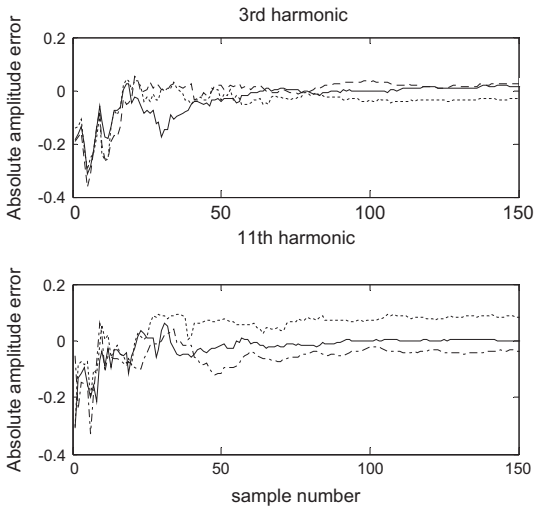

Fig. 3b. Comparison of 3rd and 11th harmonic amplitude error with 20 dB noise. - - - -, UKF; – – –, MPSO; —, APSO.

Table 3
Absolute error of frequency-modulated signal with 20 dB noise.

Order of harmonic	UKF	MPSO	APSO
Fundamental freq. error (Hz)	0.0538	0.0501	0.0046
Fundamental amp. error (pu)	0.055	0.0452	0.0028
3rd Harmonic amp. error (pu)	0.081	0.071	0.0086
5th Harmonic amp. error (pu)	0.0818	0.0575	0.0039
11th Harmonic amp. error (pu)	0.046	0.0258	0.0105

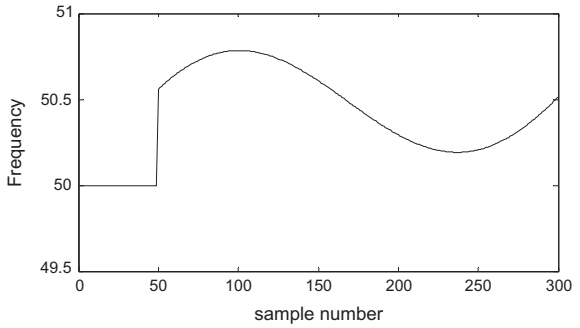

Fig. 4a. Modulated frequency change.

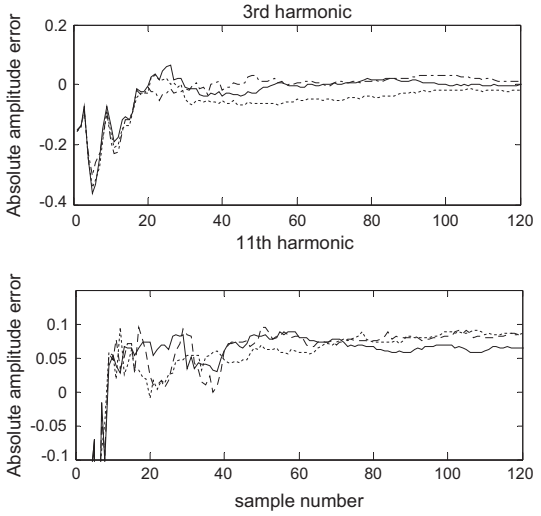

Fig. 4b. Comparison of 3rd and 11th harmonic amplitude error with 20 dB noise. - - - -, UKF; – – –, MPSO; —, APSO.

The absolute estimation error for the fundamental frequency and amplitude of different harmonic components is presented in Table 2. From this table it is quite evident that the UKF and its optimized variants exhibit less estimation error in comparison to the EKF filter. In a similar way Figs. 3a and 3b depict the ramp frequency change and absolute error in amplitude tracking of 3rd and 11th harmonic components using UKF, MPSO and APSO, respectively.

4.3. Frequency-modulated signal

In this case the nominal frequency of the signal is modulated with 1 Hz and 6 Hz signals represented in the following way:

$$fr(k) = \{fr0 + \sin(2\pi k T_s) + 0.5\sin(12\pi k T_s)\} \quad (43)$$

where $fr, fr0$, and k represent the modulated frequency, mean frequency, and sample count, respectively. The test signal in this case is the same as given in Eq. (43), and absolute error in frequency and amplitude for the fundamental, 3rd, 5th, and 11th harmonics are shown in Table 3, respectively. From the table it is observed that the frequency and harmonic amplitude errors are very small in the case of APSO algorithm in comparison to all other

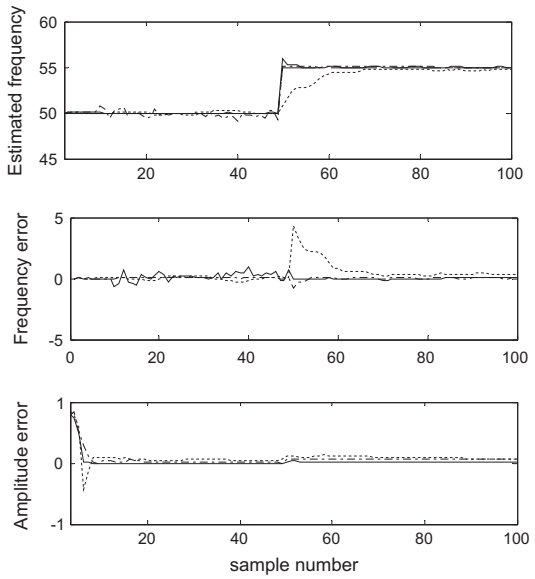

Fig. 5. Comparison of fundamental frequency and amplitude error with 20 dB noise. - - - -, UKF; – – –, MPSO; —, APSO.

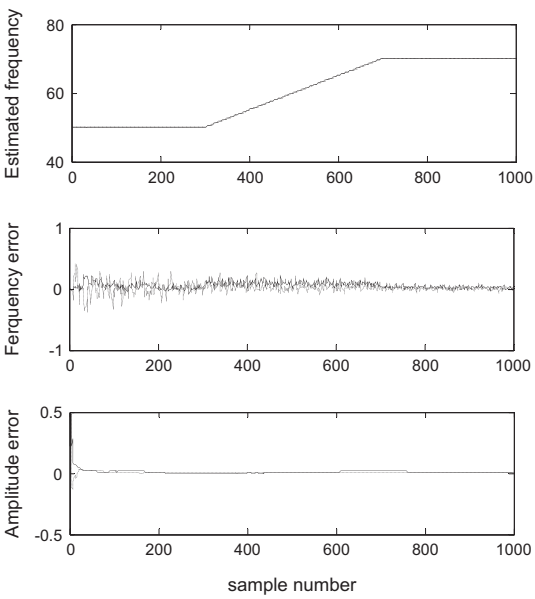

Fig. 6. Comparison of UKF and AUKF with 20 dB noise. - - - -, UKF; —, TUKF.

filtering algorithms presented in this paper. Figs. 4a and 4b depict the modulated frequency change and absolute error in amplitude tracking of 3rd and 11th harmonic components using UKF, MPSO and APSO, respectively.

4.4. Step change in system frequency

A sudden change of fundamental frequency by 5 Hz is initiated at the 50th sampling instant on the test signal which is mixed with 20 dB of white Gaussian noise and the performance of the unscented filter is evaluated for APSO algorithm. Fig. 5 depicts the tracking performance of both the algorithms, from which it can be seen that the APSO algorithm tracks the signal accurately in comparison to the UKF filter alone. Further the speed of response is faster in the former than the later.

Table 4
Absolute error of the signal with fundamental amplitude change and 20 dB noise.

Order of harmonic	UKF	MPSO	APSO
Fundamental amp. error (pu)	0.0149	0.0114	0.0013
3rd Harmonic amp. error (pu)	0.0241	0.0205	0.0078
5th Harmonic amp. error (pu)	0.0145	0.012	0.0037
11th Harmonic amp. error (pu)	0.015	0.009	0.0047

Table 5
Absolute error of the signal with 5th harmonic Amplitude change with 20 dB noise.

Order of harmonic	UKF	MPSO	APSO
Fundamental amp. error (pu)	0.019	0.0104	0.0001
3rd Harmonic amp. error (pu)	0.0404	0.0164	0.005
5th Harmonic amp. error (pu)	0.0277	0.0032	0.0007
11th Harmonic amp. error (pu)	0.0171	0.0112	0.0072

4.5. Performance improvement with adaptive UKF

The ramping frequency from 50 Hz to 75 Hz within a span of 400 samples is used for comparing the performance of the untuned UKF and adaptive UKF. Fig. 6 presents the performance of both these filters in the presence of noise of 20 dB and from the figure it is clearly seen that there is a significant improvement in tracking performance of the proposed filter, which is adaptively tuned and optimized. The UKF algorithm is also optimized in the same manner as the tuned UKF (TUKF).

4.6. Change in the amplitude of the fundamental component

In a similar way, the amplitude of the fundamental component is increased by 20% and the absolute error in per unit (pu) are shown in Table 4. From this table it is clearly observed that both MPSO and APSO algorithms perform the best in producing the least estimation error.

4.7. Change in the amplitude in the fifth harmonic component

The amplitude of the 5th harmonic component is then doubled from 0.15 pu to 0.3 pu, and the absolute estimation error (AE) in the 5th harmonic amplitude component is shown in Table 5 clearly revealing better performance of APSO algorithm.

4.8. Real time signal parameter estimation

Experimental test data is generated using the laboratory set up, as shown in Fig. 7. The load is fed from a 3 kV A, 230 V:230 V single-phase transformer, and the data acquisition subsystem (DAS) is activated and using another 230 V:12 V transformer. The DAS comprises a PCL-208 data

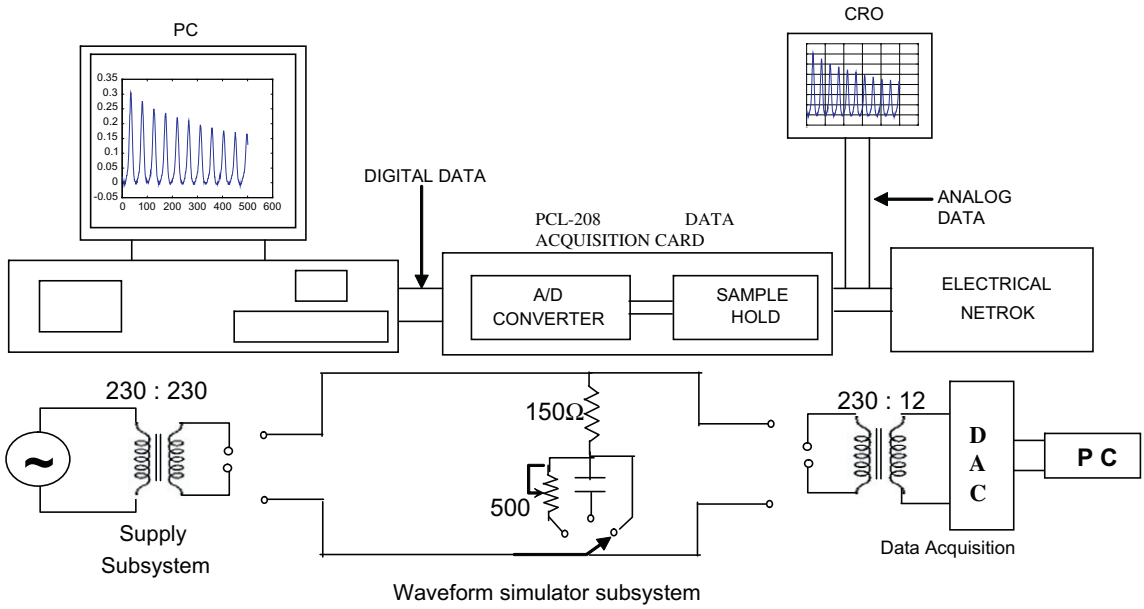

Fig. 7. Laboratory setup for simulation of time-varying signals.

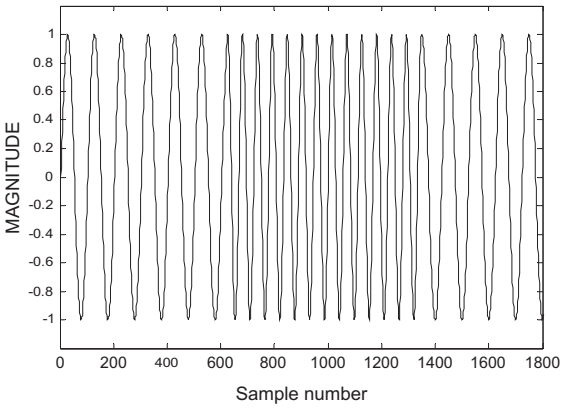

Fig. 8. Real time test signal.

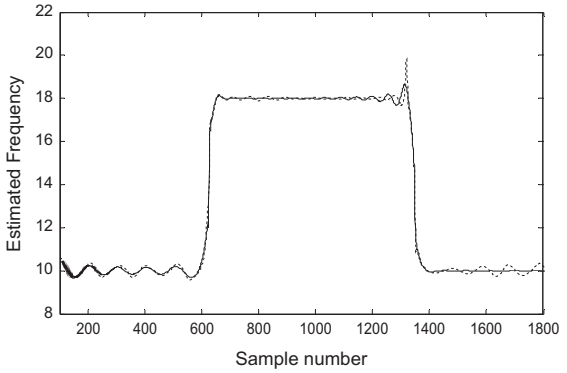

Fig. 9. Comparison of variants of PSO based UKF. – – –, MPSO; —, APSO.

acquisition card which has an inbuilt sample and hold device, and an A/D converter. The voltage across the load after transformation to 12v is sampled at a rate of 2.3 kHz and is digitized by the A/D system and the digital data is sent to PC using a program written in 'C' language. Signals with time varying amplitude and frequency are obtained using the waveform simulator by switching on and switching off the load, respectively.

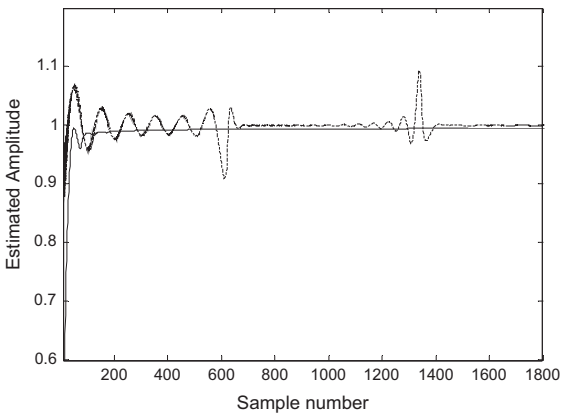

Fig. 10. Comparison of variants of PSO based UKF. – – –, MPSO; —, APSO.

For frequency estimation, the signal frequency is changed from 10 Hz to 18 Hz and then back to the initial value of 10 Hz. Fig. 8 presents the real time signal obtained from the DAS subsystem and Figs. 9 and 10 show the estimated value of the frequency and amplitude of the signal using APSO and MPSO filters, which clearly revealing the superior performance in accurately tracking the real –time test signal parameters.

5. Conclusion

In this paper, we have presented an unscented Kalman filter technique for estimation of frequency, magnitude, and phase of fundamental and harmonic components of a time-varying signal. The model and measurement error covariances of the unscented Kalman filter (UKF) are further tuned adaptively so that the filter can accurately track small or large variations in the amplitude, frequency, or phase of the signals in the presence of significant noise. Instead of trial and error method of choice of UKF parameters along with the model and measurement error covariances, an adaptive Particle Swarm Optimization techniques (APSO and MPSO) is used for the choice of optimal parameters of the filter. The effects of both the large and small variations in the amplitude and frequency of the signal are considered for computing the estimation accuracy of the proposed filter in the presence of noise. From the computer simulation results it is observed that the frequency and amplitude errors are found to be much smaller with an adaptively tuned unscented Kalman filter in comparison to the untuned one. Further the performance of the filter with optimization algorithm like APSO is found to be superior in comparison to the modified PSO (MPSO) algorithm in the estimation of frequency and harmonic magnitudes. Several simulation results confirm the efficiency of the tracking performance of this new adaptively tuned optimized unscented Kalman filter. Also experimental results for frequency and amplitude estimation of time-varying signals are presented showing the estimation accuracy of the proposed filters.

References

[1] D.W.P. Thomas, M.S. Woolfson, Evaluation of frequency tracking methods, IEEE Transactions on Power Delivery 16 (3) (2001) 367–372.
[2] A.A. Girgis, F.M. Hann, A quantitative study of pitfalls in FFT, IEEE Transactions on Aerospace and Electronic System 44 (1) (1998) 107–115.
[3] P.S. Wright, Short-time Fourier Transform and Wigner–Ville distributions to the calibration of power frequency harmonic analysis, IEEE Transactions on Instrument and Measurement 48 (2) (1999) 475–478.
[4] T.X. Zhu, Exact harmonics/interharmonics calculation using adaptive window width, IEEE Transactions on Power Delivery 22 (4) (2007) 2279–2288.
[5] L.L. Lai et al., Real-time frequency and harmonic evaluation using artificial neural networks, IEEE Transactions on Power Delivery 14 (1) (1999) 52–59.
[6] H.C. Lin, Intelligent neural network-based fast power system harmonic detection, IEEE Transactions on Industrial Electronics 54 (1) (2007) 43–53.
[7] P.K. Dash, D.P. Swain, A.C. Liew, S. Rahman, An adaptive linear combiner for on-line tracking of power system harmonics, IEEE Transactions on Power Systems 11 (4) (1996) 1730–1735.

[8] Y.N. wang, J.C. Gu, C.M. Cheu, An improved adaline algorithm for on-line tracking of harmonic components, International Journal of Power and Energy Systems 23 (2) (2003) 117–125.
[9] H.C. So, P.C. Ching, Adaptive algorithm for direct frequency estimation, Proc. Inst. Elect. Eng., Radar Sonar Navig. 151 (6) (2004) 359–364.
[10] H.C. So, K.W. Chan, Y.T. Chan, K.C. Ho, Linear prediction approach for efficient frequency estimation of multiple real sinusoids: algorithm and analysis, IEEE Transactions on Signal Processing 53 (7) (2005) 2290–2305.
[11] J.Z. Yang, C.S. Yu, C.W. Liu, A new method for power signal harmonic analysis, IEEE Transactions on Power Delivery 20 (2) (2005) 1235–1239.
[12] S.Y. Xue, S.X. Yang, Power system frequency estimation using supervised Gauss–Newton algorithm, Measurement 42 (2009) 28–37.
[13] Jian Yang, Hongsheng Xi, Wei Guo, Robust modified Newton algorithm for adaptive frequency estimation, IEEE Transactions on Signal Processing Letters 14 (11) (2007) 879–882.
[14] H.C. So, A comparative study of three recursive least squares algorithms for single-tone frequency tracking, Signal Processing 83 (9) (2003) 2059–2062.
[15] A.K. Pradhan, A. Routray, A. Basak, Power system frequency estimation using least mean square technique, IEEE Transactions on Power Delivery 20 (3) (2005) 1812–1816.
[16] M. Bettayeb, U. Quidiani, A hybrid least squares-GA based algorithm for harmonic estimation, IEEE Transactions on Power Delivery 18 (2) (2003) 52–67.
[17] S. Mishra, Hybrid least squares adaptive bacterial foraging strategy for harmonic estimation, IEE Proc:-Gener. Transm. Distrib. 152 (3) (2005) 379–389.
[18] A. Routray, A.K. Pradhan, K.P. Rao, A novel Kalman filter for frequency estimation of distorted signals in power system, IEEE Transactions on Instrumentation and Measurement 51 (3) (2002) 469–479.
[19] F.F. Costa, A.J.M. Cardoso, D.A. Fernandes, Harmonic analysis based on Kalman filtering and Prony's method, in: Proc. Int. Conf. Power Engineering, Energy Electrical Drives, Setúbal, Portugal, April 12–14, 2007, pp. 696–701.
[20] T.W. Hilands, S.C.A. Thomopoulous, Nonlinear filtering methods for harmonic retrieval and model order selection in Gaussian and non-Gaussian noise, IEEE Transactions on Signal Processing 45 (4) (2004) 163–195.
[21] E.A. Wan, R. Van der Merwe, The unscented Kalman filter for non-linear estimation, in: Proc. IEEE Symposium 2000 (AP-SPCC), Lake Louise, Albenta, Canada, October, 2000.
[22] K. Xiong, H.Y. Zhang, C.W. Cham, Performance evaluation of UKF-based nonlinear filtering, Automatica 22 (2006) 261–270.
[23] S. Julier, J. Uhlmann, H.F. Durrant-Whyte, A new method for the nonlinear transformation of means and covariances in filters and estimators, IEEE Transactions on Automatic Control 45 (2000) 477–482.
[24] Zhe Jiang, Qi Song, Yuqing He, Jianda Han, A novel adaptive unscented Kalman filter for nonlinear estimation, in: 46th IEEE Conference on Decision and Control, New Orleans, LA, USA, December 12–14, 2007.
[25] S.J. Julier, J.K. Uhlmann, Unscented filtering and nonlinear estimation, Proceedings of the IEEE 92 (3) (2004) 401–422.
[26] J. Kennedy, R.C.Eberhart, Particle swarm optimization, in: Proc. IEEE Int. Conference on Neural Network., Piscataway, NJ, IEEE Press, 1995, pp. 1942–1948.
[27] Zhang Liping, Y. Huanjun, Chen Dezhao, Hu Shangxu, Analysis and improvement of particle swarm optimization algorithm, Information and Control 33 (5) (2004) 513–517.
[28] R.C. Eberhat, Y. Shi, Comparing inertia weight and constriction factors in particle swarm optimization, in: Proc. of the IEEE Congress on Evolutionary Computation, IEEE Press, San Diago, CA, 2000, pp. 84–88.
[29] Z. Lu, T.Y. Ji, W.H. Tang, Q.H. Wu, Optimal harmonic estimation using a particle swarm optimizer, IEEE Transactions on Power Delivery 23 (2) (2008) 1166–1174.